What regulates electron injection in diffusive shock acceleration?

Siddhartha Gupta[1], Damiano Caprioli[1,2] & Anatoly Spitkovsky[3]

1. Department of Astronomy and Astrophysics, University of Chicago, IL 60637, USA
2. Enrico Fermi Institute, University of Chicago, IL 60637, USA
3. Department of Astrophysical Sciences, Princeton University, 4 Ivy Ln., Princeton, NJ 08544, USA

Abstract

Collisionless shocks are one of the most efficient sources for energetic nonthermal particles. Although the microphysics of proton acceleration is revealed to some extent, the exact mechanisms that channel a fraction of thermal electrons to nonthermal population are still not fully understood.

The key open questions are

- What are the crucial processes and threshold condition that determine electron injection in diffusive shock acceleration (DSA)?
- How does the acceleration efficiency depend on the shock speed ($v_{\rm sh}$), Alfvén Mach number ($M_{\rm A} = v_{\rm sh}/v_{\rm A}$), and the sonic Mach number ($M_{\rm s} = v_{\rm sh}/v_{\rm th}$)?
- What are the effects of upstream magnetic field inclination ($\theta_{\rm Bn}$)?

To develop a comprehensive theory of electron acceleration, we have performed a survey of fully kinetic non-relativistic shock simulations in spatially 1D geometry using the massively parallel electromagnetic Particle-In-Cell code, Tristan-MP. The results are crucial to understand the nonthermal phenomenology of a variety of heliophysical and astrophysical collisionless shocks from interstellar space to galaxy clusters.

Journey from thermal to nonthermal

Low Mach number shock

- Electrons escape from the shock.
- Acceleration stalls.

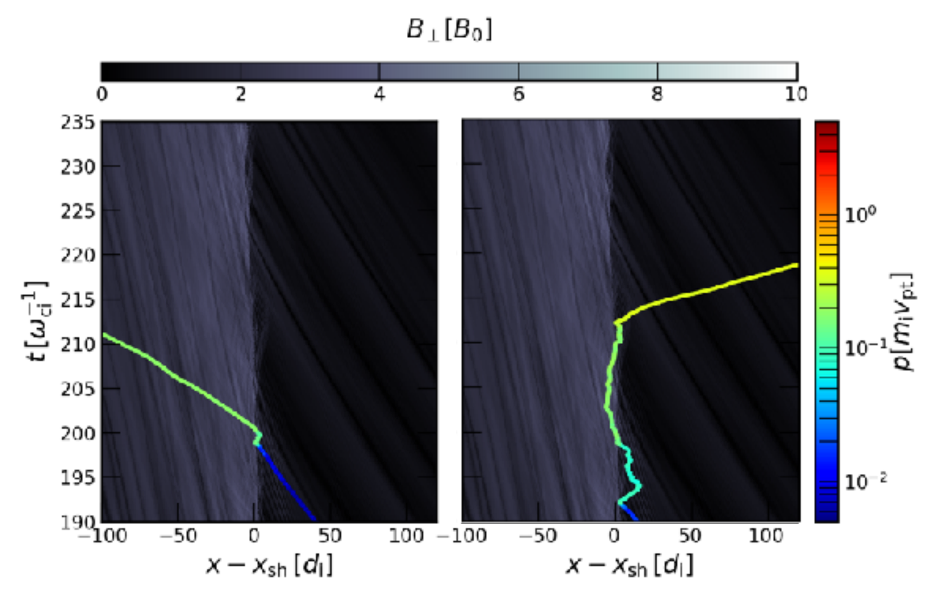

Figure 3. Trajectory of two tracer electrons in $M_{\rm A} = 5$ shock.

High Mach number shock

- Particles are confined near the shock.
- Maximum energy is increasing.

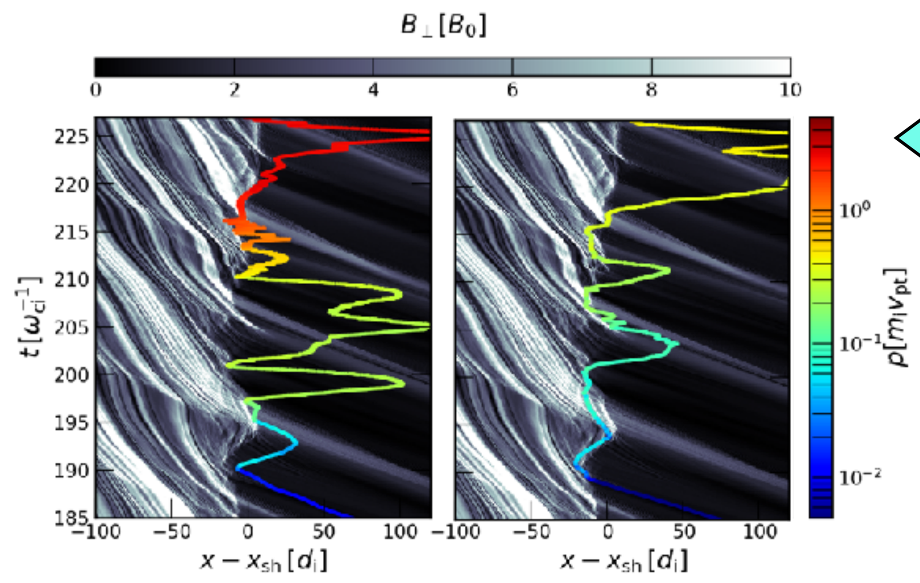

Figure 4. Trajectory of two tracer electrons in $M_{\rm A} = 20$ shock.

Shock structure

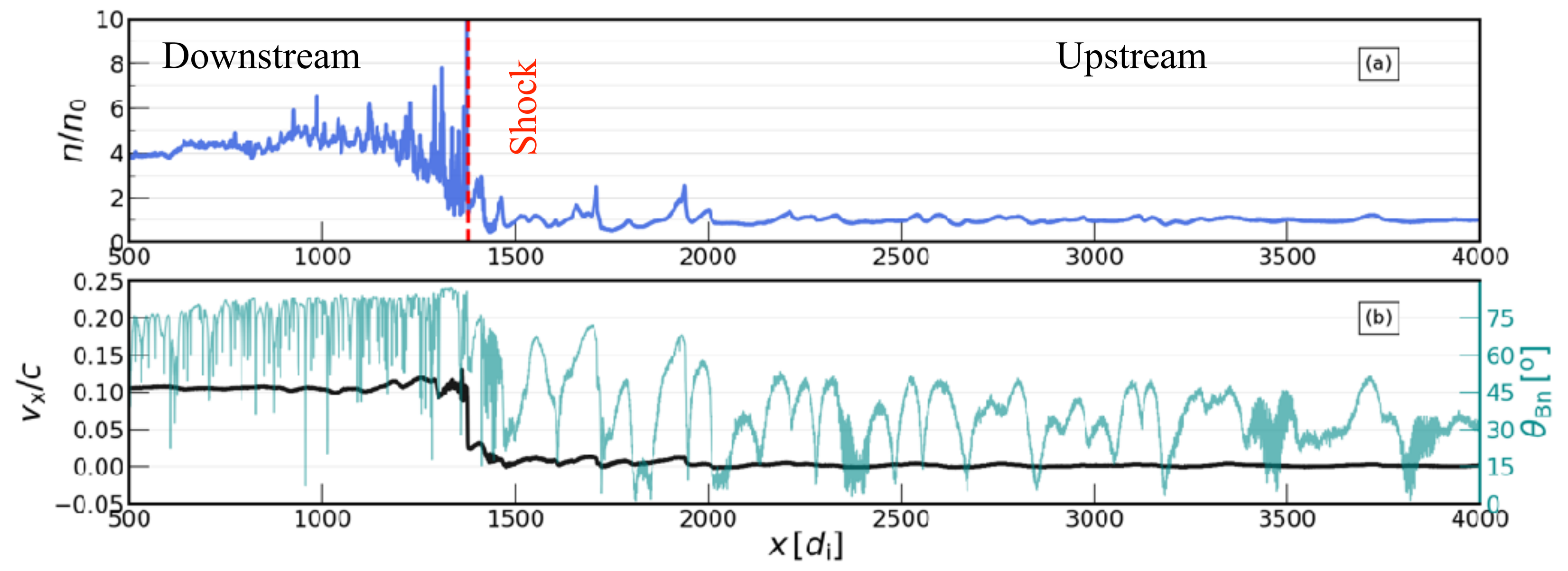

Figure 1. Profiles of density, the x-component of the plasma speed, and the effective shock inclination $\theta_{\rm Bn} = \cos^{-1}(B_x/|\mathbf{B}|)$ at $t = 275\,\omega_{\rm ci}^{-1}$. Run parameters: $v_{\rm pt}/c = 0.1, M_{\rm A} = 20, M_{\rm s} = 40$, and $m_{\rm i}/m_{\rm e} = 100$.

Our investigation focuses on quasi-parallel shocks, where the inclination of the upstream **B** field relative to shock normal is initialized with $\theta_{\rm Bn} = 30^{\rm o}$. Shock is launched using a piston moving at a speed $v_{\rm pt}$ in the upstream frame.

- Plasma (thermal + cosmic rays) density profile is similar to MHD shocks.
- Interactions between thermal and energetic particles produce instabilities.
- Self-generated electromagnetic turbulence re-arranges $\theta_{\rm Bn}$.

Dependence on Mach number

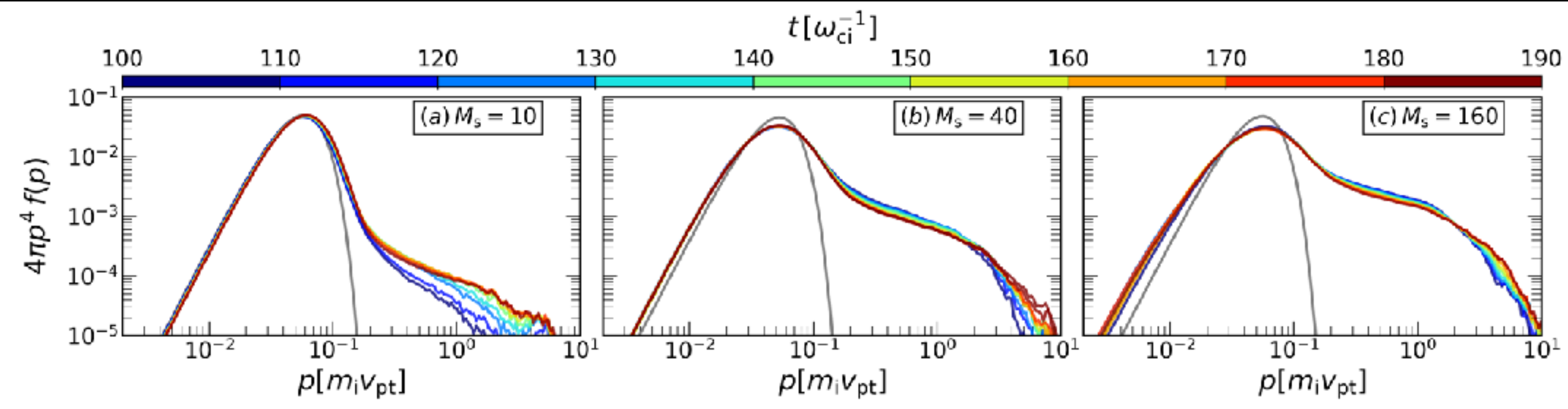

Figure 5. Downstream electron spectra for $M_{\rm s} = 10, 40$, and 160 shocks (electron sonic Mach numbers 1, 4, and 16 respectively)

- Acceleration works for both subsonic and supersonic electrons.
- Nonthermal fraction reduces with smaller $M_{\rm s}$ shocks.
- Low $M_{\rm A}$ shocks show a cut-off at smaller momentum $p/(m_{\rm i}v_{\rm pt})$.
- High Mach number shocks accelerate electrons to highest energies.

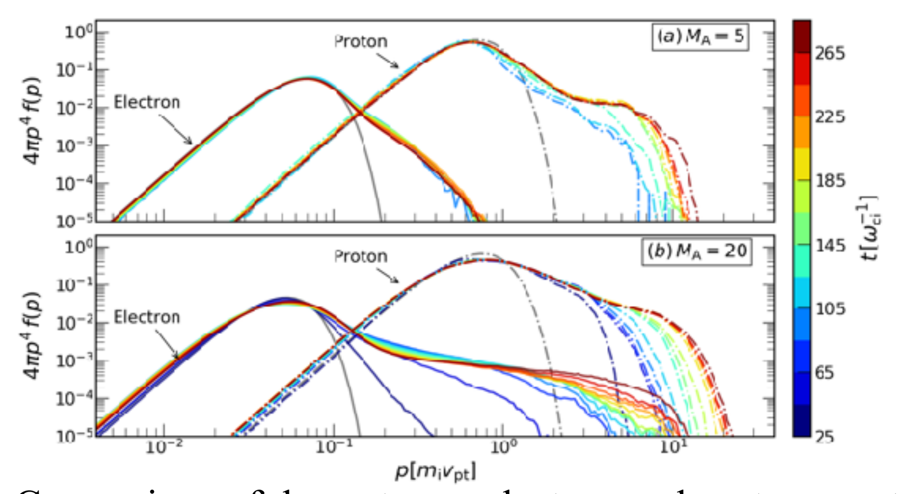

Figure 6. Comparison of downstream electron and proton spectra between $M_{\rm A} = 5$ (panel a) and $M_{\rm A} = 20$ (panel b) shocks.

Momentum distribution and spectra

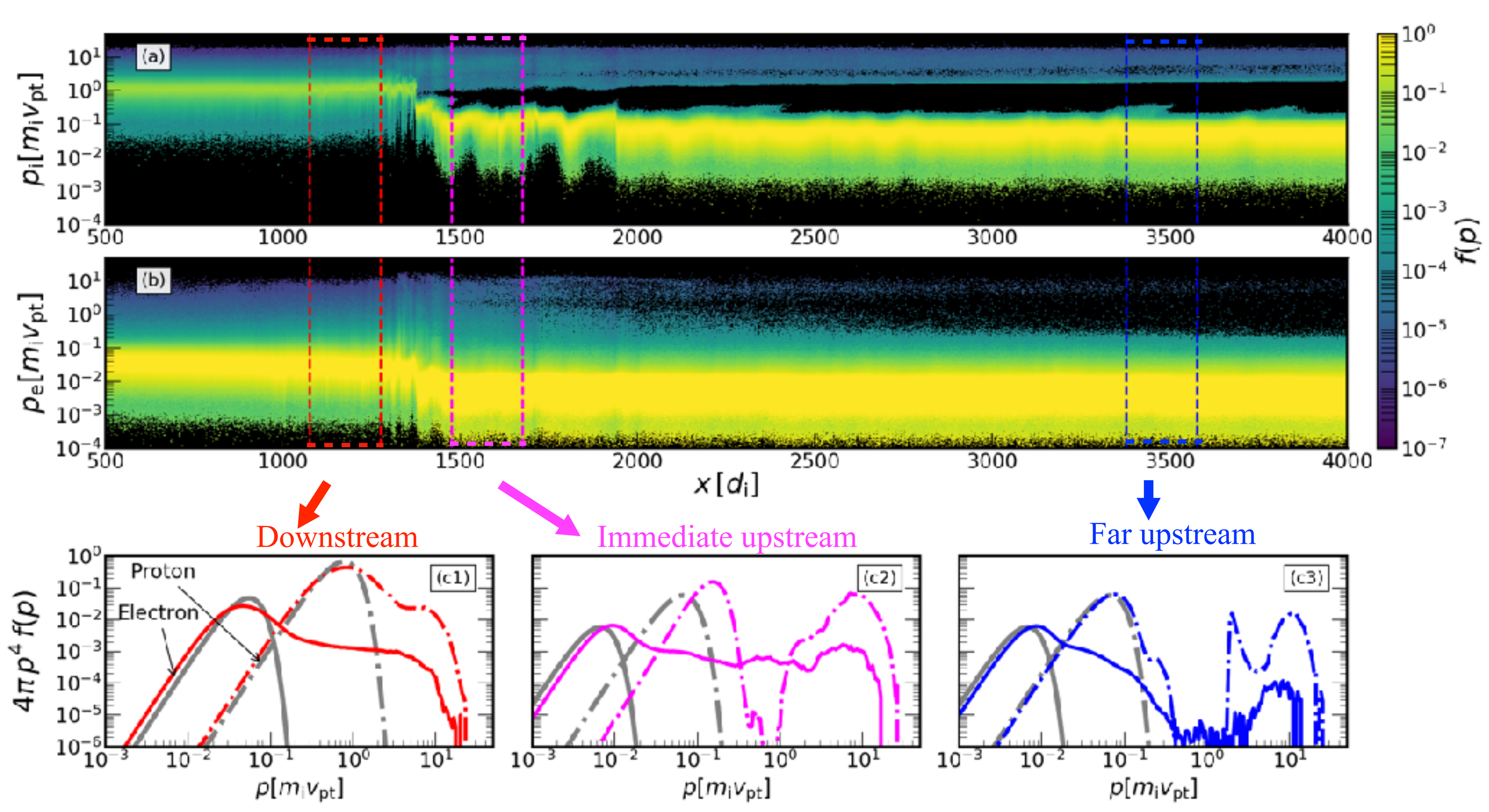

Figure 2. The $x - |\mathbf{p}|$ diagram at $t = 275\omega_{\rm ci}^{-1}$. Panels (a) and (b) stand for proton and electron, respectively. Panels (c1)-(c3) represent the spectra of protons (dash-dotted line) and electrons (solid line).

- Upstream proton distributions contain thermal and nonthermal populations.
- The electron distribution is made of three populations: thermal, current compensating super-thermal, and nonthermal electrons.

Summary

- Non-relativistic quasi-parallel shocks can produce nonthermal electrons efficiently (e.g., Figs 1and 2).
- Reflectivity of a shock and the electromagnetic fluctuations both are crucial for electron DSA injection (Figs 3 and 4).
- Subsonic electrons can also participate in the DSA (Fig 5).
- Due to lack of large-amplitude modes in low $M_{\rm A}$ shocks, the spectra show cut-off at smaller energies (Figs 3 and 6).
- In high Mach number shocks, the nonthermal tail keeps growing to higher energies (Figs 4 and 6).

References including:

1. Arbutina, B., & Zekovi´c, V. 2021, Astroparticle Physics, 127, 102546
2. Caprioli, D., Pop, A., & Spitkovsky, A. 2015, ApJL, 798, 28
3. Guo, X., Sironi, L., & Narayan, R. 2014, ApJ, 794, 153
4. **Gupta, S., Caprioli, D. & Spitkovsky, A., in prep.**
5. Morris, P. J., Bohdan, A., Weidl, M. S., & Pohl, M. 2022, ApJ, 931, 129
6. Park, J., Caprioli, D., & Spitkovsky, A. 2015, PRL, 114, 085003
7. Shalaby, M., Lemmerz, R., Thomas, T., & Pfrommer, C. 2022, ApJ, 932, 86
8. Spitkovsky, A. 2005, in AIP Conf. Proc. 801, Astrophysical Sources of High Energy Particles and Radiation.

Contact: gsiddhartha@uchicago.edu

For latest updates:
www.siddharthagupta.com

38th International Cosmic Ray Conference (ICRC2023), 26 July - 3 August, 2023, Nagoya, Japan